batteries

Article

A Fast Prediction of Open-Circuit Voltage and a Capacity Estimation Method of a Lithium-Ion Battery Based on a BP Neural Network

Wenkang Bao, Haidong Liu, Yuedong Sun and Yuejiu Zheng *

College of Mechanical Engineering, University of Shanghai for Science and Technology, Shanghai 200093, China
* Correspondence: yuejiu.zheng@usst.edu.cn

Abstract: The battery is an important part of pure electric vehicles and hybrid electric vehicles, and its state and parameter estimation has always been a big problem. To determine the available energy stored in a battery, it is necessary to know the current state-of-charge (SOC) and the capacity of the battery. For the determination of the battery SOC and capacity, it is generally estimated according to the Electromotive Force (EMF) of the battery, which is the open-circuit-voltage (OCV) of the battery in a stable state. An off-line battery SOC and capacity estimation method for lithium-ion batteries is proposed in this paper. The BP neural network with a high accuracy is trained in the case of sufficient data with the new neural network intelligent algorithm, and the OCV can be accurately predicted in a short time. The model training requires a large amount of data, so different experiments were designed and carried out. Based on the experimental data, the feasibility of this method is verified. The results show that the neural network model can accurately predict the OCV, and the error of capacity estimation is controlled within 3%. The mentioned method was also carried out in a real vehicle by using its cloud data, and the capacity estimation can be easily realized while limiting inaccuracy to less than 5%.

Keywords: lithium-ion battery; open-circuit voltage; capacity estimation; BP neural network

check for updates

Citation: Bao, W.; Liu, H.; Sun, Y.; Zheng, Y. A Fast Prediction of Open-Circuit Voltage and a Capacity Estimation Method of a Lithium-Ion Battery Based on a BP Neural Network. *Batteries* **2022**, *8*, 289. https://doi.org/10.3390/batteries8120289

Academic Editors: Yanan Wang, Chengshan Xu, Carlos Ziebert and Xiaogang Wu

Received: 17 November 2022
Accepted: 13 December 2022
Published: 16 December 2022

1. Introduction

With the continuous consumption of non-renewable energy, more and more energy problems are emerging. Most countries in the world coincidentally focus their development on the extraction and storage of renewable energy [1]. As an important energy storage device, batteries can store electricity from one of the many renewable energy sources for use at other times. Lithium-ion batteries are also used in various fields because of their large capacity and long cycle life. The rapid development of the electric vehicle industry has undoubtedly benefited from lithium-ion batteries as well [2]. However, one of the many problems affecting the large-scale promotion of electric vehicles is the estimation of battery capacity, because the battery capacity can visually reflect the battery health, and the capacity estimation can also be used to study their cycle life [3–5]. As the power source of electric vehicles, the state of the battery directly affects the operation of EVs. Due to the different manufacturing conditions and use environments, the same type of battery will experience different degrees of aging, and, thus, the battery capacity will gradually decrease. The battery capacity is directly related to the electric vehicle range, and inaccurate capacity estimation will incorrectly display the range available, greatly affecting the user experience. Although, most electric vehicles are equipped with a battery management system (BMS) that can properly manage the batteries in the vehicle [6]. However, its accuracy for battery capacity estimation is still in the stage of needing improvement and refinement. If the method of performing the complete charging and discharging process of the entire vehicle battery to arrive at the capacity is used, it is obviously too cumbersome.

In order to reduce the time needed for capacity estimation and ensure a certain level of confidence, a new method needs to be proposed to achieve fast capacity estimation.

As understood from the internal chemicals of the battery [7], the capacity of the battery decays continuously with the increasing number of cycles in use [8], so the capacity estimation is often linked to the battery aging condition [9–11]. The use of empirical models such as the Arrhenius aging model [12–14] can simulate the battery aging state more intuitively, thus allowing for accurate capacity estimation under simple operating conditions, and there are also many studies that optimize on the basis of this aging model to achieve a wide use of empirical models [15,16]. However, the increasing complexity of the model makes practical application more difficult. The hybrid neural network proposed in the literature [17] combines a convolutional neural network and bidirectional long-short-term memory network model to realize battery monitoring and prediction. Combining the model with algorithms places a high demand on mathematical knowledge. Commonly used data-driven approaches based on data analysis are also proposed when the focus is placed on data analysis rather than the mechanism itself. Associating battery aging with specific characteristics such as the differential voltage [18] and the incremental capacity curve [16,19–21], the peak position and amplitude of the curve are analyzed to determine the current capacity [22]. Some studies have adopted both model- and data-driven methods. In [23], the author developed a residual capacity estimation method based on mechanism- and data-driven models which require both mathematical analysis and optimization algorithms.

The state of charge of the battery is often used for capacity estimation. The ratio of the change of charge and discharge to the change of the corresponding SOC is often used to calculate the capacity, which is shown in Equation (1). In Equation (1), C_{cap} indicates the calculated capacity, t_1 and t_2 are the two moments before and after the battery is charged, SOC_1 and SOC_2 are the SOC of the battery at these two moments, respectively. I represents the current and η = 1 represents the coulomb efficiency. In this method, the cumulative electricity between two different SOCs is also calculated. If SOC_1 and SOC_2 under different times, t_1 and t_2, can obtained, the electric quantity change can be calculated by integrating the current between t_1 and t_2. So, the capacity can be estimated by these conditions. This paper adopts the closed-loop method, which is simple and easy to implement. In the process of implementation, the BP neural network plays a key role. The rapid development and maturity of neural networks has also contributed to the battery SOC and capacity estimation. In [24], the dual-dropout-based neural network proposed by the authors considers the influence of the battery use process by the operation of the whole vehicle from many perspectives and finally achieves the multi-step SOC prediction of the battery.

$$C_{cap} = \frac{\int_{t_1}^{t_2} \eta * I_t dt}{SOC_1 - SOC_2} \tag{1}$$

Another advantage of calculating the capacity based on Equation (1) is that it takes a short time and is less affected by the error caused by the accumulation of current. The key point lies in the acquisition of two SOCs. The SOC is often associated with the battery capacity estimation, so an accurate SOC estimation has also become one of the research focuses. SOC estimation methods are commonly divided into two categories. The first type is based on battery voltage, current and internal resistance, such as the open-circuit voltage method [25], ampere-hour integration method and estimation method based on battery internal resistance. The other category is more novel and intelligent algorithms, mainly including the Kalman filter method [26–29], neural network, support vector machine, etc. The open-circuit voltage (OCV) method is mainly based on the relationship between the SOC and OCV in the battery characteristics. This method can obtain the SOC faster, but in practical applications, it is rare to obtain the open-circuit voltage directly, because the voltage needs a period of relaxation after the charging and discharging stops to reach the open-circuit voltage. A method of predicting the OCV in a short time is proposed in [30], which enhances the degree of applicability of the open-circuit voltage method.

The open-circuit voltage is an important parameter of lithium-ion batteries, and its acquisition method usually requires the battery to be set aside for a long time after charging and discharging [31]. It often takes several or tens of hours. As Figure 1a shows, a–c is the discharge process, and the voltage drops. The current stops in c, and the voltage stops both in a,b and c,d, which shows the ohmic characteristics of the battery. The relaxation process d,e and voltage rise slowly and finally stabilize. The red part of the Figure can be used for capacity estimation, and the specific flow is given in Figure 1b. The battery management system applied in the vehicle can achieve a more accurate sampling of the battery terminal voltage, so the collected terminal voltage can also be used for the capacity estimation of the real vehicle.

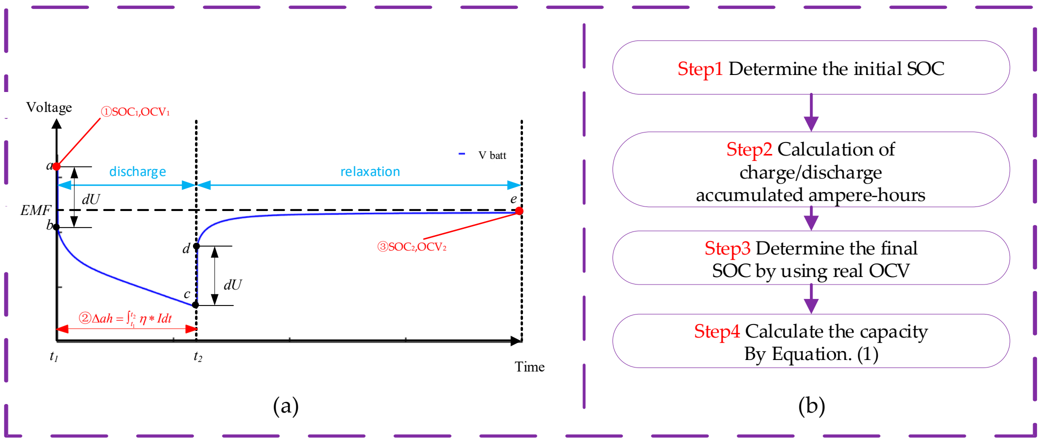

Figure 1. (**a**) The relaxation curve variation process of the cell; (**b**) Battery capacity estimation process.

Many methods for inferring the OCV through mathematical algorithms and models have also been proposed [32,33], but the shortcoming of such methods is the need for timely parameter calibration. In reference [34], the authors extracted reliable characteristics from the relaxation voltage curves of 130 lithium-ion batteries under several cycle conditions to build a dataset and construct a model to achieve the battery capacity estimation. In [35], the voltage variation of the battery relaxation process was analyzed from an electrochemical point of view by the internal chemical reaction mechanism, and a nonlinear structural model of the battery relaxation process after charging was established, but the corresponding analysis of the discharge case was missing. In [36], a model containing the particle size distribution of active materials was used to physically explain the phenomenon of slow relaxation, and the reason why the battery relaxation process in the experiment was shorter than that in the model was analyzed. However, the capacity estimation work was not further advanced. In [37], a new voltage relaxation model was proposed, which, based on diffusion theory and the theory of electrochemical reaction, achieves fast OCV prediction for lithium-ion batteries at a high SOH (state of health). This model greatly reduces the time needed for calculation and is relatively simple, but it is not applicable to batteries with a low SOH. It is still necessary to study the methods for predicting the OCV in a short time, and that can be applied to cells in various situations.

At present, many studies mainly focus on battery SOC and capacity estimation. Whether it is a mechanistic model or a data-driven method, the ultimate goal is to obtain the SOC or to directly obtain the battery capacity. Many factors, such as the model accuracy and battery usage, can lead to inaccurate battery capacity estimation results. The accurate models are also difficult to apply in practice because of the complexity of building, the large number of calculations and the high requirement for mathematical knowledge. The relationship between the open-circuit voltage and battery SOC is well established and not influenced by other factors, so it can be directly used for capacity estimation. However, the difficulty of obtaining the OCV makes many studies prohibitive, so few studies have been conducted to analyze the open-circuit voltage of the battery after charging and discharging. In this paper, the OCV is taken as the research object to realize the accurate and fast prediction of stable OCV. By using the accurate relationship between the OCV and SOC, the battery SOC can be accurately located, and the capacity of the lithium-ion battery can be accurately estimated. The proposed method does not require an understanding of the battery mechanism and model building, and there are no complex mathematical formulas and algorithms required, which is a simple, fast and accurate capacity estimation method, and the general flow chart of the method is given in Figure 2.

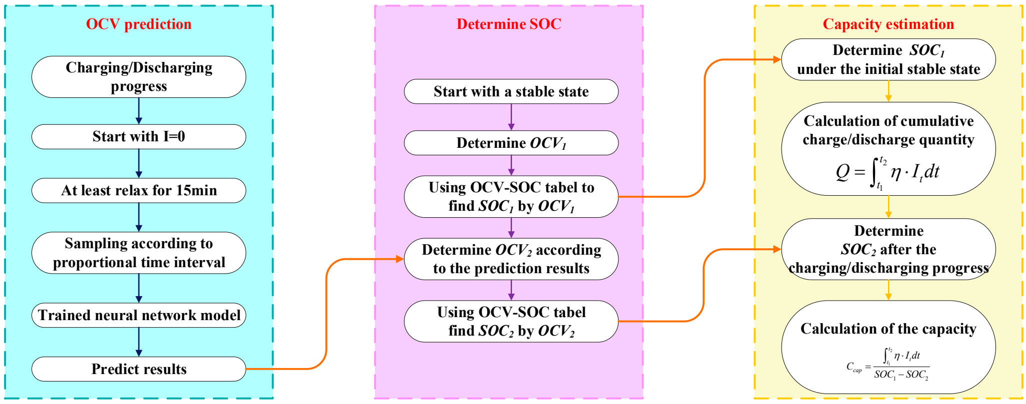

Figure 2. Schematic diagram of capacity estimation.

The rest of this article is organized as follows. In Section 2, the proposed method is elaborated on in detail. In Section 3, the battery tests are introduced. The method validation and discussions are outlined in Section 4. Conclusions are finally drawn in Section 5.

2. Capacity Estimation Method

2.1. Capacity Estimation Procedure

In the case of a large amount of data, the proposed neural network method requires the information of the terminal voltage variation of the battery during a short period of resting as the training data and as the input of the neural network and the open-circuit voltage of the battery after a long period of resting as the output. The completed neural network model is used to achieve fast OCV estimation for a single cell. The cell that uses this method to estimate the capacity needs to meet certain conditions. First, the cell needs to be charged and discharged in a stable state, and the open circuit voltage in this stable state is denoted as OCV_1. An OCV-SOC curve can be obtained through the calibration method between the OCV and SOC of the cell, and the same type of battery can share a curve. This correspondence is relatively linear, and the OCV under different SOCs can be obtained by the interpolation method. However, the OCV-SOC curve of the LFP battery is relatively flat at the middle SOC [38], as shown in the blue box in Figure 3b. The error is larger using the open-circuit voltage capacity estimation method. In contrast, the NCM battery OCV–SOC curve is better characterized with a large OCV difference between different SOCs, as shown in Figure 3a, and is more suitable for capacity estimation by this method. The SOC in this state can be obtained from the stable OCV_1 through the corresponding relationship, denoted as SOC_1. According to Equation (1), it needs to obtain the SOC_2, which can also be obtained by looking up the table. Therefore, the question is to find the open-circuit voltage of the battery after charging and discharging, namely, OCV_2. The BP neural network method proposed later in this paper can quickly predict OCV_2, so the capacity estimation can be realized. This method requires that the SOC_1 or SOC_2 should not be too large or too small in order to avoid the error caused by the variation in the OCV–SOC curves after battery aging. The OCV–SOC curve of the aging battery will deviate from that of the fresh battery at low and high SOCs. In view of the inaccurate capacity estimation caused by this problem, the following suggestions are made: (1) to recalibrate the aging battery; (2) to use a relatively accurate medium SOC value for evaluation. Given the complexity of the recalibration of aged batteries in real vehicles, the proposed method (2) is used in the paper. The neural network prediction method proposed in this paper can reduce the capacity estimation time to within half an hour with high accuracy.

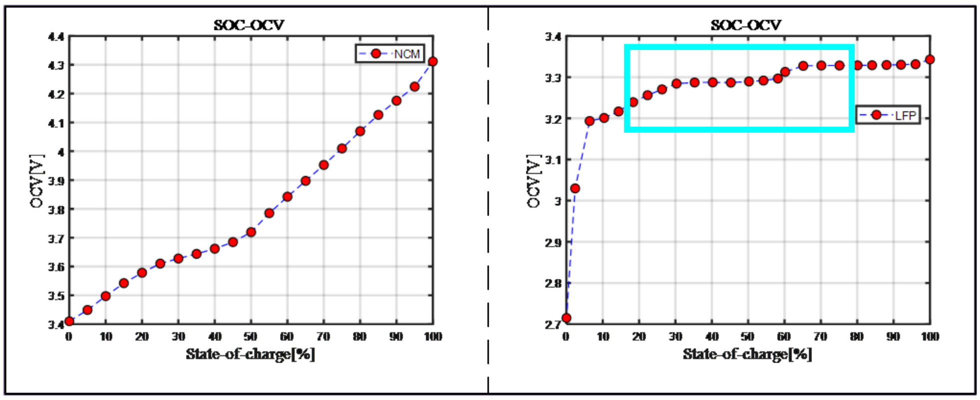

Figure 3. OCV–SOC curve of the battery. (**a**) NCM battery; (**b**) LFP battery.

2.2. BP Neural Network

A Back Propagation (BP) neural network is a kind of neural network widely used at present. As a multi-layer feedforward neural network trained according to the error back propagation algorithm, it systematically solves the problem of learning the connection rights of network implicit elements. The BP neural network also refers to neural networks that use backpropagation algorithms. The reverse transfer in the algorithm actually transfers the calculated prediction error, and the weight and threshold between each layer are adjusted in time according to the error size in the model. Therefore, a complete process includes two parts: the forward propagation of the input data and the backward propagation of the error. The neural network usually consists of an input layer, a hidden layer and an output layer, as shown in Figure 4. The terminal voltage at short relaxation times is used as the network input, and the stable open-circuit voltage is selected as the output label. The neural network is trained by a large amount of data, which eventually makes the network learn the characteristics of voltage variation and obtain the optimal weight parameter matrix and BP neural network model, which can simply implement the stable open-circuit voltage prediction.

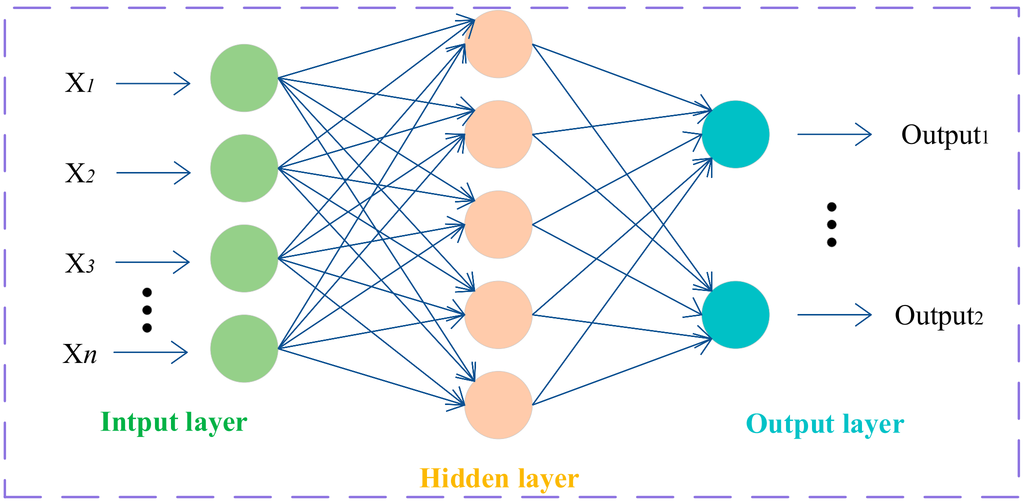

Figure 4. Structure diagram of the neural network model.

The advantage of the BP neural network is that there is no need to determine the mathematical relationship between the input and output; there is only a need to provide data for training and learning, and the accuracy of the prediction results is positively related to the amount of training data. At the same time, the model adopts the gradient descent method in the process of parameter optimization to minimize the value of the objective function, and the network convergence is controlled within a suitable range by an adaptive learning rate. The internal signal propagation mode includes the forward propagation of the signal and the backward propagation of the error. When the error is large, the network will carry out back propagation, and the error is transmitted from the output layer to the input layer through the hidden layer and then averaged to each neuron, and the neuron adjusts the weights and thresholds according to the gradient descent algorithm. Through repeated training and iterations until the output error is less than the set value, the training is finished, and the successfully trained network can predict the value similar to the actual value with the input of new samples. The whole process can be divided into two stages: the network training and the prediction process. The specific steps are shown in Figure 5.

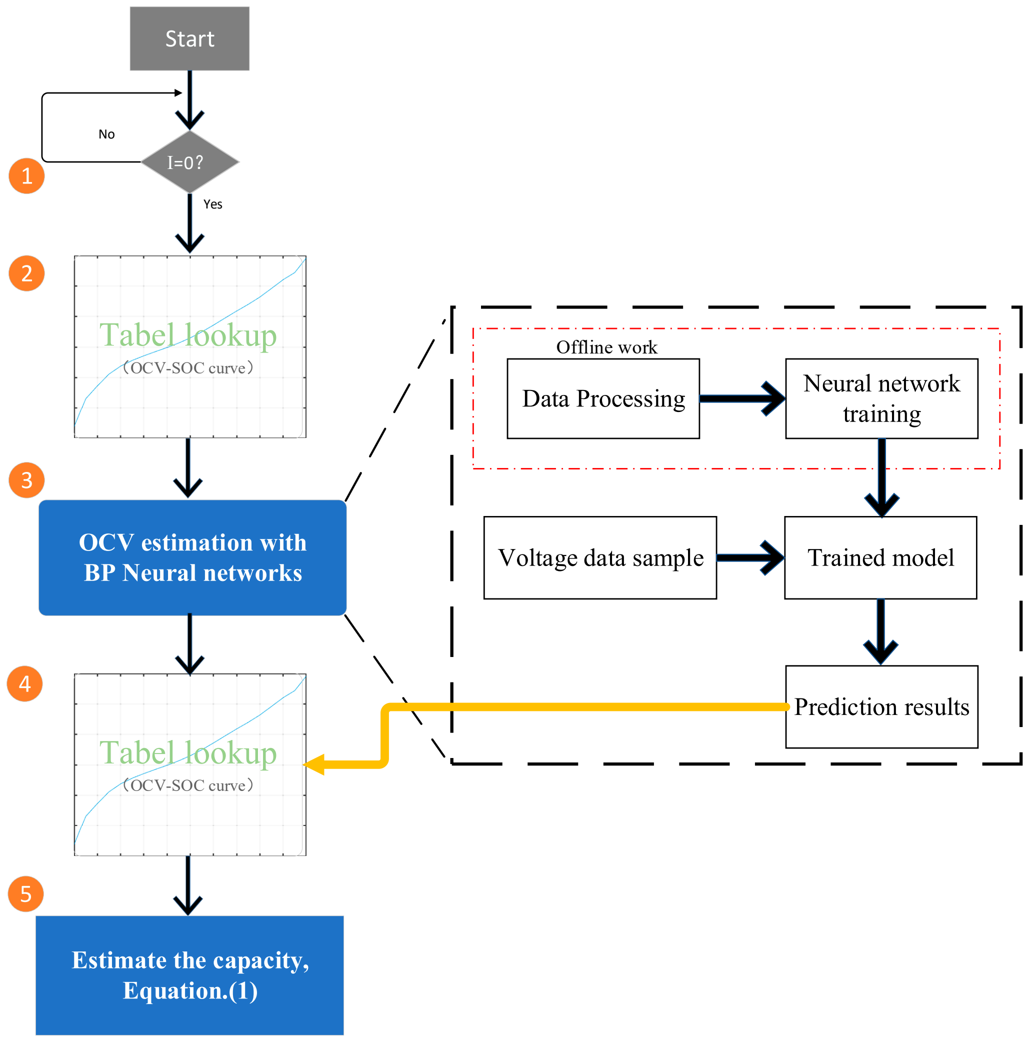

Figure 5. Flowchart of rapid capacity estimation based on a BP neural network.

Given a training set, $x^i = [v_1^i, v_2^i, \ldots, v_{15}^i]$ is a set of input vectors. $y^i = [v_t^i]$ is an output vector; $i = 1, 2, \ldots,$ n means the number. All inputs and outputs constitute the whole dataset $D = (X,Y)$, which is given in Equation (2).

$$X = \begin{bmatrix} v_1^1 & v_2^1 & \cdots & v_{15}^1 \\ v_1^2 & v_2^2 & \cdots & v_{15}^2 \\ \vdots & \vdots & \ddots & \vdots \\ v_1^n & v_2^n & \cdots & v_{15}^n \end{bmatrix}, \ Y = \begin{bmatrix} v_t^1 \\ v_t^2 \\ \vdots \\ v_t^n \end{bmatrix} \tag{2}$$

2.3. Selection and Processing of Datasets

The purpose of a BP neural network is to fit the voltage relaxation curve and finally predict the stable open-circuit voltage based on the short-time information of terminal voltage when the battery is resting. The dataset consists of the experimental data of Cell1 to Cell3 mentioned in Section 3. After the experiment, the relaxation voltage information of the three batteries under different operating conditions was collected.

It is not necessary to use all the voltage during the short-time relaxation period. Its complexity needs to be minimized while satisfying the prediction accuracy of the neural network. Therefore, a method is proposed for sampling the terminal voltage for a short period of time when the battery is resting. The voltage values of 15 points are sampled as the characteristic voltages, the sampling period is an unbalanced period and the sampling method is to collect in an equal proportional series incremental way, with time as the interval. Because when the circuit is in the initial open state, the voltage changes rapidly and the sampling frequency is relatively high, with the increase in time, the voltage change rate slows down and the sampling period increases. The battery voltage is extracted according to the interval time t, where t = 3, 6, 9, 15, 21, 33, 45, 69, 93, 141, 189, 285, 381, 573 and 765, and the sampling time is controlled within 900 s. The extracted 15 voltages can not only describe the voltage variation in the process of cell relaxation, but they can also occupy less calculation space and are convenient for training. Figure 6 shows the voltage sampling diagram. The voltage changes rapidly within 0–200 s, and the sampling frequency is high. The voltage changes slowly within 300–900 s, so the sampling frequency is relatively low. An accurate OCV requires a resting time of at least 2 h, and there may still be a difference of tens of mV between the voltage at the sampling point and the actual OCV. Therefore, a large amount of data training is required to achieve accurate prediction.

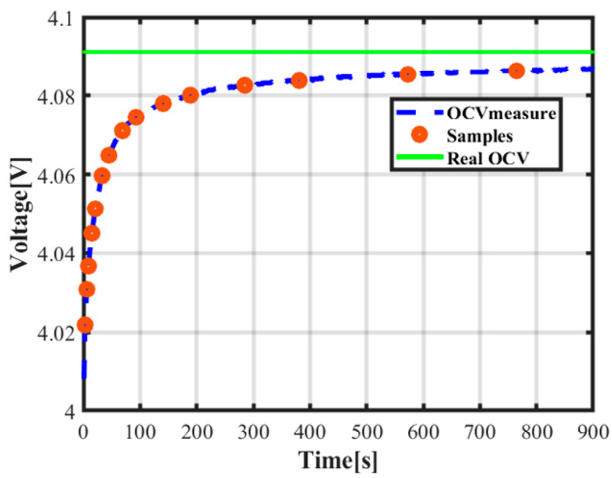

Figure 6. Schematic diagram of 15 voltage samples.

2.4. The Process of the BP Neural Network Design and Construction

The structure of the BP neural network is mainly determined by the number of input points, the number of hidden layer layers, the number of hidden layer neurons, the output nodes and the activation function. The dataset is fifteen feature values to predict one final stable open-circuit voltage, and this neural network is a multi-input single-output network. The single-layer hidden layer network node has strong nonlinear mapping ability and a fast network convergence speed, so the single-hidden-layer structure is chosen in this paper. Too many neurons in the hidden layer will affect the learning efficiency, even leading to overfitting. Otherwise, the network training effect is not good enough. The number of neurons in the general hidden layer is given by the empirical Equation (3). *S* is the number of nodes in the hidden layer, *M* is the number of neurons in the input layer, *N* is the number of neurons in the output layer and *A* is a constant between 1 and 10. According to the empirical formula, the value range of the number of neurons in the hidden layer is 5–14. Here, the number of neurons in the hidden layer is 10. In this paper, the *tansing* function is used as the hidden layer activation function, and the *purelin* function is used as the output layer activation function. The structure of the final open-circuit voltage prediction neural network is shown in Figure 7.

$$s = \sqrt{m+n} + a \tag{3}$$

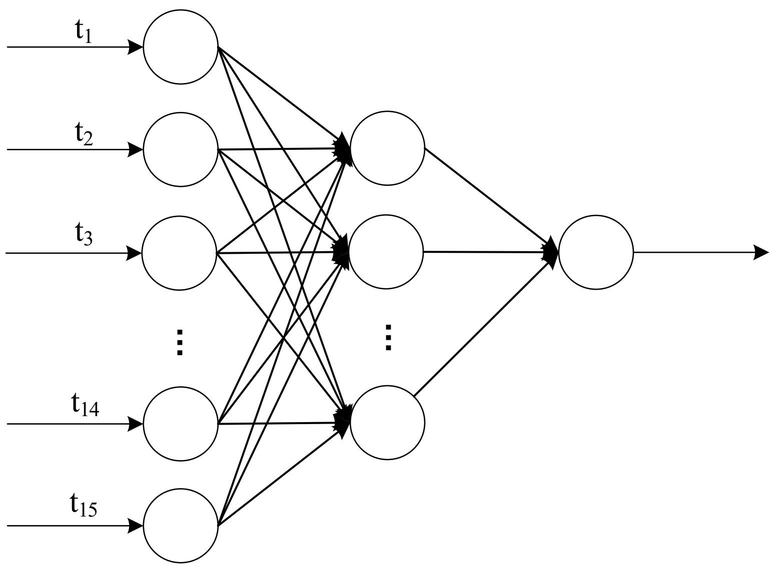

Figure 7. Structure diagram of an open-circuit voltage prediction neural network.

The following step is to train the BP neural network model *net** and solve the optimal neural network model for dataset *D* and the optimal weight parameter matrix set *W** for each layer of the network. *net*: $X \to Y$ means the model constructed from the dataset *D*. *W*: $X \to Y$ means the weight parameter matrix of each layer in neural network is given by Equation (4). W^l, l = 2, . . . , L is the weight parameter matrix from layer L-1 to layer L of the BP neural network, where the weight parameter already contains the bias term of each layer. The *i*th sample error can be expressed as Equation (5). The cumulative error on the dataset is expressed as Equation (6). The BP neural network model is trained according to dataset *D* such that the error of the model should reach the minimum value according to the preset minimum value. For the sample data (x^i,y^i), its objective function is shown as Equation (7).

$$W = \left\{W^2, W^3, \ldots, W^L\right\} \tag{4}$$

$$Loss(net(x^i), y^i, W) = \frac{1}{2}\left|\left|net(x^i) - y^i\right|\right|^2 \tag{5}$$

$$R = \sum_{i=1}^{n} Loss(net(x^i), y^i, W) \tag{6}$$

$$\text{argmin}R = Loss(net(x^i), y^i, W) \tag{7}$$

The initial value of the weight parameter matrix W is randomly initialized in the range of (0,1), and the parameter matrix is iteratively updated on the dataset D; t represents the number of iterations. The weight parameter obtained from the previous sample data is used as the initial weight parameter of the next sample data until the stopping condition is reached. The optimal weight parameter matrix of each layer in the BP neural network model constructed from the final dataset D is W_*^l. At the meantime, the optimal weight parameter matrix set W_* and the optimal network model net_* are obtained.

3. Experimental

The experiments mainly include basic experiments and the specifical cycle experiments in order to obtain more datasets. The basic experiments are the nominal capacity experiment and the battery aging experiment. The nominal capacity experiment is the key to obtaining an accurate battery capacity to verify the accuracy of the capacity estimation of this method. The aging experiment is only for specific batteries to verify whether the proposed method is also applicable to aging batteries. In this paper, the commonly used cylindrical lithium-ion battery is taken as the research object. The five batteries produced by the same manufacturer are named cell1, cell2, cell3, cell4 and cell5, respectively, and the cathode material is NCM. Cell1~cell3 was used as the source of the model training set, and cell4 was used for method verification. Cell5 was used to verify the application of the method to an aging battery. The basic cell parameters are given in Table 1, and the experiment introduction is shown in Table 2. The specific parameters of the experimental equipment used are shown in Table 3. The computer is installed with corresponding program software to analyze and process the data. The type of the battery test system is HYNN-CT05200F. The channel of this experimental bench was used for charging and discharging experiments on batteries, and the data recording frequency was 1 Hz.

Table 1. Basic performance parameters of the battery.

Items	Specifications
Positive and negative electrode materials	NCM/C
Normal capacity (Ah)	3.1
Normal voltage (V)	3.6
Charge/discharge cut-off voltage (V)	4.1/2.5
Nominal charging mode	CC-CV
Operating temperature (°C)	Charge −10~45/Discharge −20~60

Table 2. The experimental arrangement.

Number	The Experimental Scheme	Temperature
Cell1~Cell4	Charge/discharge-rest cycle	10 °C~25 °C~45 °C
Cell5	Cycle of aging	25 °C

Table 3. Experimental equipment.

Number	Equipment	Manufacture	Indicators
1	PC	Lenovo	
2	Charge and discharge machine	Neware	0–5 V, 0–1 mA
3	Thermostat	Bell	−40–150 °C

3.1. Basic Tests

The nominal capacity experiment is carried out first. First, the temperature is set at 25 °C, and the battery is connected to the device and left to stand for 3 h so that the battery is in a completely stable state. Then, the battery was discharged until the voltage drops to the cut-off voltage, and then the battery was left to rest for 1 h. The battery is fully charged by constant current–constant voltage (CC–CV) and rests for an hour. After three cycles of these two steps, the real capacity can be calculated by the average capacity of these cycles.

To verify whether this method has the same effect on aging cells, the aging test was conducted on cell5. The aging experiment consists of a nominal capacity experiment and a small cycle of aging decay. The steps of the small cycle are as follows: adjust the battery to a high SOC, discharge at a 1 C rate for 10 min, leave it for 3 h, discharge the battery to 0% SOC at a 1 C rate with a constant current (CC), charge the battery to 100% SOC at a 1/3 C rate with a constant current and constant voltage (CC-CV) and continue to adjust the battery SOC to different values of a high SOC. The next step is to adjust different high SOC levels and repeat the discharge–charge process 10 times. The battery is attenuated 100 times in total, with a nominal capacity test every 10 times.

3.2. Specific Experiments

In order to achieve the requirement of large datasets and at the same time ensure the robustness of the network, it is required to charge and discharge the battery under different charge/discharge ratios, temperatures and SOCs. The temperature is set at 10 °C, 25 °C and 45 °C in order to obtain the relaxation information of the battery at different temperatures. The SOC includes low, medium and high ranges. All of the settings are designed to simulate the different use situations of real vehicles. The detailed experimental steps are given in Table 4. In the experiment, a three-hour rest period is given after each charging and discharging process. The purpose is to obtain the voltage data used in Section 2.3 and 4. The final stable open-circuit voltage can also be obtained by this experiment. Finally, as many data as possible can be obtained for neural network training. These data contain the relaxation information of the battery under different conditions.

Table 4. Detailed operation steps of the specific cycle.

Steps	Specifications
Step 1	Set the temperature at 25 °C.
Step 2	Adjust the SOC to a high SOC.
Step 3	Discharge at 1 C for 10 min, and rest for 3 h.
Step 4	Charge at 1 C for 10 min, and rest for 3 h.
Step 5	Adjust the SOC to a medium SOC. Repeat the steps from 3 to 4.
Step 6	Adjust the SOC to a low SOC. Repeat the steps from 3 to 4.
Step 7	Repeat the steps from 2 to 6 with 0.5 C and 2 C current.
Step 8	Set the temperature at 10 °C and 45 °C. Repeat the steps from 2 to 6.

After specific experiments, a total of 352 groups of sample data were collected. The samples were divided into 80% as the training set, 10% as the validation set and the other 10% as the test set. The final training dataset is shown in Table 5.

Table 5. Sampling dataset.

Number	t1	t2	…	t14	t15	Target
1	3.9074	3.9152	…	3.9837	3.9849	3.9890
2	3.7555	3.7630	…	3.8247	3.8268	3.8498
3	3.6092	3.6163	…	3.6796	3.6811	3.6889
4	3.4985	3.5057	…	3.5773	3.5788	3.5847
5	3.3575	3.3665	…	3.4542	3.4595	3.4747
6	3.8482	3.8560	…	3.9195	3.9205	3.9239
7	3.6982	3.7056	…	3.7670	3.7695	3.7921
8	3.5624	3.5692	…	3.6309	3.6318	3.6359
9	3.4421	3.4495	…	3.5345	3.5382	3.5481
10	3.2753	3.2899	…	3.3717	3.3742	3.3823
…	…	…	…	…	…	…
352	3.2592	3.2769	…	3.3640	3.3661	3.3739

4. Results and Discussion

4.1. Predicted Results of the OCV

According to the dataset obtained from the experiment, the neural network is trained. Figure 8 shows the convergence graph of the BP neural network, the minimum output error is 2.1192×10^{-5} and the number of iterations is 70. The network convergence speed is fast, and the convergence accuracy is very high. The regression analysis of the BP neural network model on three different datasets and the whole data is shown in Figure 9. It can be seen that the experimental data results are stable, and the relevant composite coefficients between the predicted value and the real value on the three datasets are very close to 1, which means that the model is trained well.

The trained model is now used to perform OCV prediction on the unlabeled data to verify the applicability of the network model. The experimental data of Cell4 is used. According to the open-circuit voltage prediction procedure, 15 characteristic voltage values are extracted according to the initial curve of terminal voltage relaxation and input to the trained network model, and the corresponding prediction results are obtained directly. Then, the predicted OCV was compared with the real OCV obtained from long-time rest. The comparison between the true and predicted values is given in Figure 10.

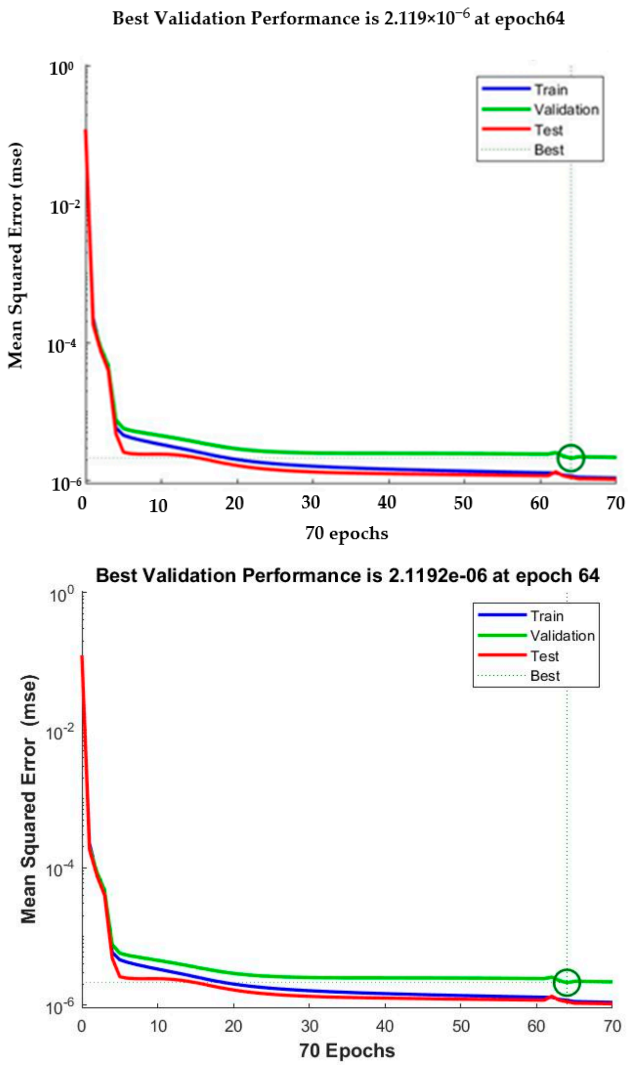

Figure 8. Convergence of the BP neural network.

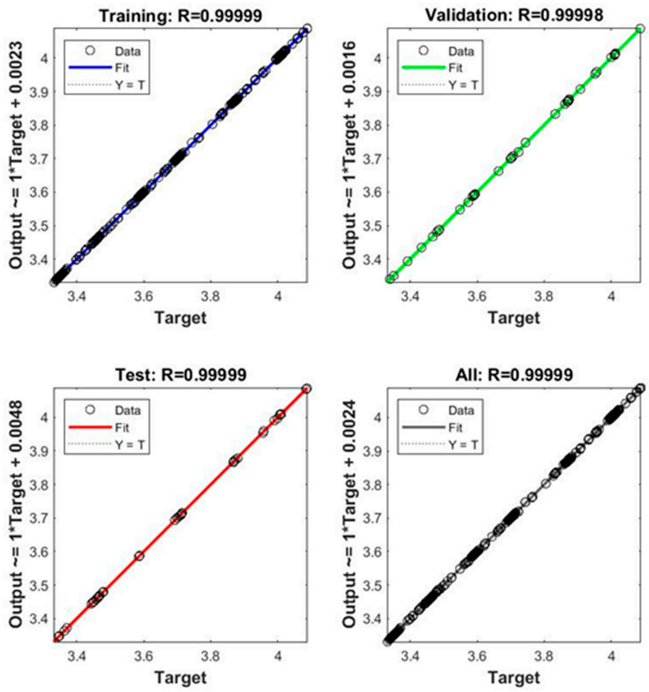

Figure 9. Analysis of the BP neural network regression.

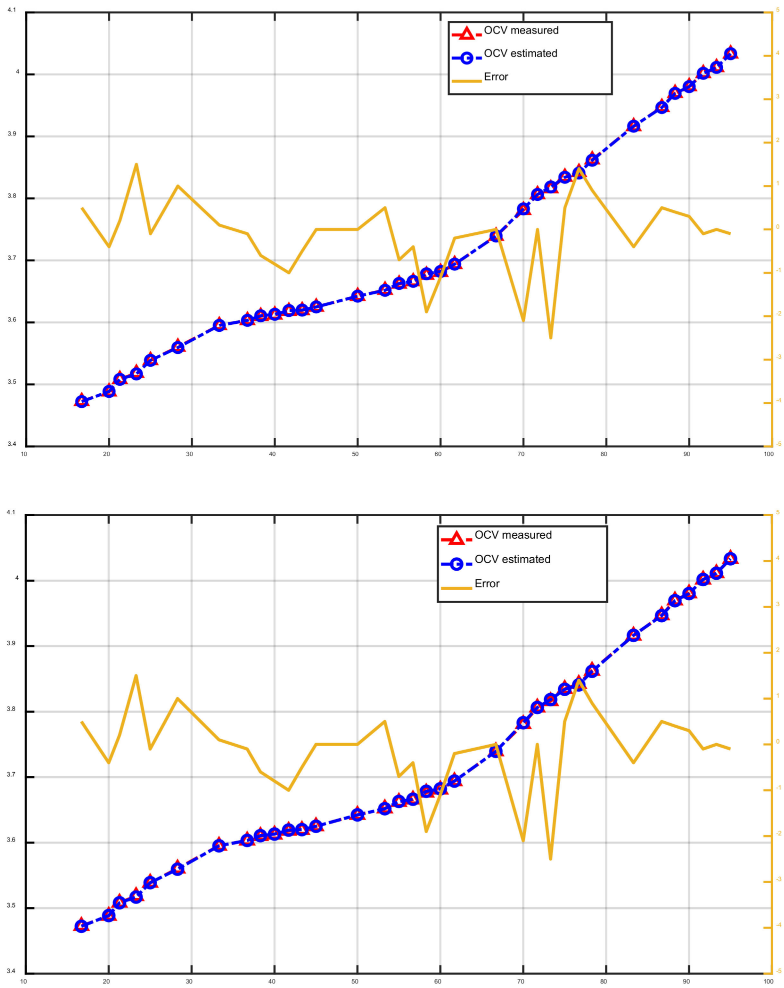

Figure 10. The prediction results of the BP neural network.

In Section 3.2, the OCV of cells at different SOCs are known, so, here, the predicted OCVs are compared with the actual values to see the accuracy. The prediction results cover the SOC range from 15% to 95%. It can also be seen that the actual OCV under different SOCs is close to the predicted value. The yellow curve on the graph represents the error between the predicted results and the actual OCV. It can be seen that the overall error is within 5 mV, which shows that the prediction is good. Based on the trained neural network model, the final stable open-circuit voltage of the battery can be predicted quickly.

In order to verify the open-circuit voltage estimation results of the aging cell cell5, the open-circuit voltage estimation results after 20, 30, 50, 70 and 100 aging cycles are selected, which are shown in Table 6. It can be seen that the open-circuit voltage of the battery after varying degrees of aging is still accurate, so the method proposed in this paper is not affected by battery aging.

Table 6. Stable open-circuit voltage prediction results after aging cycles.

Cycles	Initial SOC	Real OCV/V	Estimation/V	Error/mV
20	81.212%	3.8227	3.8216	1.1
30	82.694%	3.8354	3.8345	0.9
50	83.576%	3.8452	3.8431	2.1
70	84.4%	3.8541	3.8529	1.2
100	83.5129	3.8406	3.835	2.4

4.2. SOC and Capacity Estimation

The open-circuit voltage of the battery can be obtained through the prediction model of the BP neural network. According to the process in Figure 4, the SOC and the capacity of the battery are estimated according to the capacity estimation method. The results of the battery capacity estimation under several different SOCs are shown in Table 7.

Table 7. Capacity and SOC estimation results.

Name	Result 1	Result 2	Result 3	Result 4	Result 5
Initial OCV_1 (V)	3.9509	3.9034	3.6657	3.8028	3.8550
Initial SOC_1 (%)	86.21	77.58	52.36	60.89	67.32
Changed Ah	0.5	0.5	0.5	0.5	0.5
Predicted OCV_2 (V)	3.8053	3.7562	3.5886	3.6231	3.6949
Real OCV_2 (V)	3.8061	3.7558	3.5876	3.6238	3.6938
OCV prediction error (mV)	0.7	0.4	1.0	0.7	1.1
Estimated SOC_2 (%)	69.84	60.71	35.93	44.5	50.9
Changed SOC (%)	16.37	16.87	16.43	16.39	16.42
Estimated capacity (Ah)	3.154	3.063	3.144	3.151	3.145
Real capacity (Ah)	3.1	3.1	3.1	3.1	3.1
Capacity estimation error (Ah)	0.054	0.037	0.044	0.051	0.045
Percentage of capacity estimation error (%)	1.8	1.2	1.5	1.7	1.5

The results show that the error of OCV prediction based on the BP neural network is generally within 3 mV. Accurate OCV prediction can ensure the accuracy of SOC estimation such that the capacity calculation is more precise. The percentage of the capacity estimation error also remained within 3%. A detailed analysis of the capacity estimation is made for the first set of data results. First, the initial OCV_1 obtained by the equipment is 3.9509 V, and the SOC_1 determined by looking up the OCV–SOC relationship table is 86.21%. The calculated discharge capacity of the battery for 10 min is 0.5 Ah. Second, 15 characteristic voltages extracted from the battery resting section were introduced into the trained BP neural network model. The predicted OCV_2 was obtained, which is 3.8053 V. Compared with the real OCV 3.8061 V, the prediction error was 0.7 mV; then, through the look-up table, the SOC_2 was determined to be 69.84%. Finally, the calculated capacity is 3.054 Ah; compared with the actual capacity of 3.1 Ah, the difference is 0.046 Ah, and the estimated error is 1.4%.

4.3. Validation of Methods in Cloud Data

In order to verify the applicability of this method to real vehicle data, the BMS cloud data stored in the cloud systems currently set up by major manufacturers for their own production passenger cars were selected for validation. Although the frequency of cloud data recording is low, the relevant charging and resting data after processing can be applied to evaluate the performance of automotive power batteries. The cloud capacity estimation schematic is shown in Figure 11. The data from the real vehicle during operation and charging conditions are recorded by the internal system and uploaded to the cloud database. If the data stored in the cloud are pre-processed and trained by a neural network model using the method in this paper, the stranded OCV and thus the capacity can be accurately estimated.

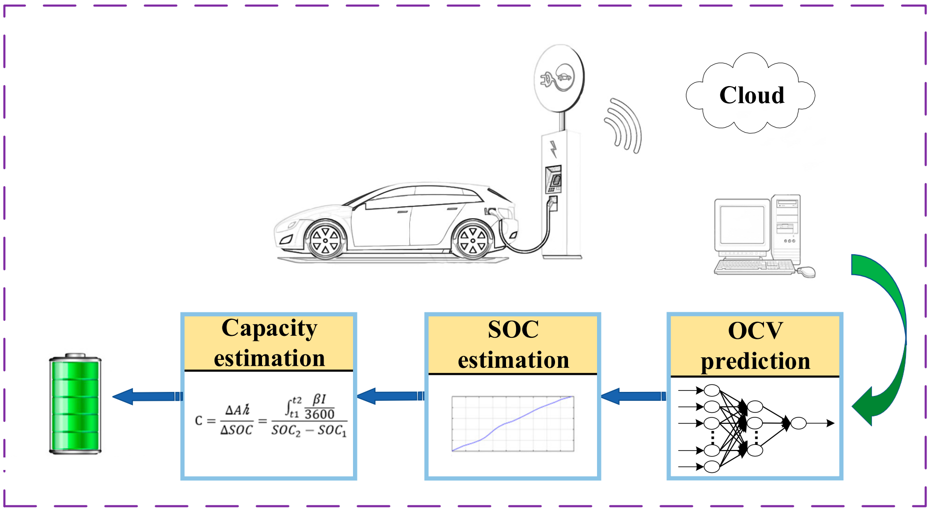

Figure 11. Capacity estimation process in the cloud data.

The data used in this section are from the cloud data of an operational vehicle. For the single cell that has only experienced a short time (a few minutes or ten minutes) in the cloud data, a BP neural network model is established to quickly predict the open-circuit voltage. Figure 12 gives the length of time and the number of times the vehicle rested after charging in the cloud record. It is not difficult to see that the rest time of the car after charging is relatively long; the data are ideal and can be used for model training. This model is trained from a total of 360 sets of resting voltage data for the first 20 times for all single cells.

Because the used battery pack in this car is composed of hundreds of single cells, it takes time to study all of the hundreds of cells. Therefore, this paper selected four cells in the battery pack for method verification, which are named cell5~cell8, respectively. Based on the trained BP neural network model and the data of this vehicle with only a short resting condition after charging, the 15 voltage values obtained from the sampling are used as the input to let the model output the OCV so as to determine the SOC of the battery at this moment by looking up the OCV–SOC table. Then, the capacity can be obtained by the calculation of Equation (1). The relevant results are shown in Table 8. The selected data have the actual OCV for comparison with the predicted values. It can be seen from the results that the prediction of OCV is still accurate, the OCV prediction error of the four selected individual cells is within 2 mV and the estimation results of the capacity are relatively accurate. The estimated capacity is close to the real capacity and is less than the nominal capacity, which shows the decay in the batteries used in the vehicle.

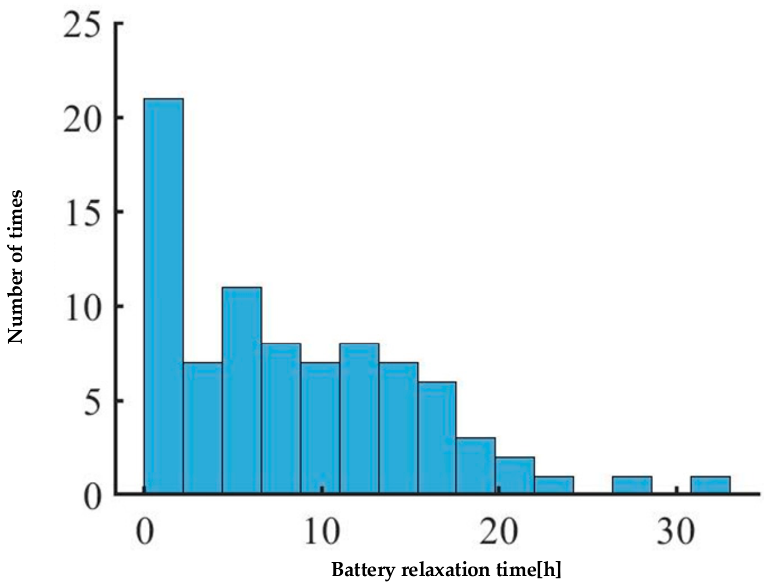

Figure 12. Length and number of relaxation times after charging.

Table 8. Results of the capacity estimation in a real vehicle.

Name	Cell 5	Cell 6	Cell 7	Cell 8
Initial OCV_1 (V)	3.28	3.28	3.284	3.283
Initial SOC_1 (%)	29.0599	29.0599	30.1978	29.9133
Changed Ah	35.91	35.91	35.91	35.91
Predicted OCV_2 (V)	3.3392	3.3338	3.3306	3.3318
Real OCV_2 (V)	3.341	3.335	3.332	3.333
OCV prediction error (mV)	1.8	1.2	1.4	1.2
Predicted SOC_2 (%)	98.7181	96.8473	93.3599	96.1544
Real SOC_2 (%)	99.3418	97.2631	96.2237	96.5702
Percentage of SOC estimation error (%)	0.6236	0.157	2.8638	0.4158
Changed SOC (%)	69.6583	67.7885	63.1622	66.2412
Predicted capacity (Ah)	51.5516	52.9774	56.8537	54.211
Real capacity (Ah)	51.0942	52.6515	54.3877	53.872
Nominal capacity (Ah)	55	55	55	55
Capacity estimation error (Ah)	0.4574	0.3259	2.466	0.339
Percentage of capacity estimation error (%)	0.9	0.62	4.5	0.63

5. Conclusions

In order to achieve a good use of batteries, it is necessary to estimate the state of batteries and evaluate the state of batteries. In recent years, with the application of cloud data, more and more EV data are uploaded to the cloud, through which the battery status can be monitored. Therefore, these recorded data can be used to estimate the SOC and capacity of the battery. Battery capacity and SOC estimation are the two core parts of battery state estimation, and other battery state estimation algorithms are also based on these two parts. The battery open-circuit voltage is closely related to SOC and can often be used for SOC estimation, but an accurate and fast method for obtaining the OCV is difficult to achieve. For the battery SOC and capacity estimation, this paper proposes a fast prediction method of OCV. The proposed BP neural network model can realize the prediction of OCV and then carries out the SOC estimation according to the OCV–SOC table, and it finally calculates the capacity according to the charge accumulation method between two points. Subject to time constraints, other cases with different SOC usage ranges are not considered. In addition, the present capacity estimation method is only applicable to NCM batteries. Subsequent work will focus on overcoming these difficulties.

The BP neural network model is used to predict the OCV. The data at the initial stage of voltage relaxation are taken as the input of the neural network, and the final stable open-circuit voltage is taken as the output of the neural network for training. Based on the experimental data, this method achieves a rapid estimation of battery capacity and controls the estimation error to within 5%. The data of the real vehicle chosen in the cloud are used to verify the proposed method, and the results are still good. However, the selected cloud data are relatively ideal because of the long relaxation time after battery charging and thus can be used for model training. All the research in this paper is based on a large number of experiments on the research object and has a lot of training data. It is no longer applicable to the case of fewer data, and the subsequent research will aim at overcoming this problem. In addition, the quality of real vehicle cloud data may be uneven, which will also affect the model training and results prediction. Specific problems need to be analyzed in detail.

Author Contributions: Software, Data curation, Validation, Writing—original draft, W.B.; Data curation, Writing—review & editing, H.L.; Supervision, Writing—review & editing, Y.Z.; Supervision, Writing—review & editing, Y.S. All authors have read and agreed to the published version of the manuscript.

Funding: This research is supported by the National Natural Science Foundation of China (NSFC) under the grant numbers of 52277222 and 52277223 and the Shanghai Science and Technology Development Fund (22ZR1444500).

Institutional Review Board Statement: Not applicable.

Informed Consent Statement: Not applicable.

Data Availability Statement: Not applicable.

Acknowledgments: The authors thank the National Natural Science Foundation of China (NSFC) under the grant numbers of 52277222 and 52277223 and the Shanghai Science and Technology Development Fund (22ZR1444500). Furthermore, the authors thank Haidong Liu, Yuejiu Zheng and Yuedong Sun for their support in the realization of the test and the method.

Conflicts of Interest: The authors declare no conflict of interest.

Abbreviations

The following abbreviations are used in this manuscript:

EV	Electric vehicle
BMS	Battery management system
SOC	State of charge
OCV	Open-circuit voltage
BP	Back propagation

References

1. Greene, D.L.; Ogden, J.M.; Lin, Z. Challenges in the designing, planning and deployment of hydrogen refueling infrastructure for fuel cell electric vehicles. *eTransportation* **2020**, *6*, 100086. [CrossRef]
2. Dixon, J.; Bell, K. Electric vehicles: Battery capacity, charger power, access to charging and the impacts on distribution networks. *eTransportation* **2020**, *4*, 100059. [CrossRef]
3. Su, L.; Wu, M.; Li, Z.; Zhang, J. Cycle life prediction of lithium-ion batteries based on data-driven methods. *eTransportation* **2021**, *10*, 100137. [CrossRef]
4. Xiong, R.; Zhang, Y.; Wang, J.; He, H.; Peng, S.; Pecht, M. Lithium-Ion Battery Health Prognosis Based on a Real Battery Management System Used in Electric Vehicles. *IEEE Trans. Veh. Technol.* **2019**, *68*, 4110–4121. [CrossRef]
5. Schmidt, S. Use of battery swapping for improving environmental balance and price-performance ratio of electric vehicles. *eTransportation* **2021**, *9*, 100128. [CrossRef]
6. Wang, X.; Wei, X.; Zhu, J.; Dai, H.; Zheng, Y.; Xu, X.; Chen, Q. A review of modeling, acquisition, and application of lithium-ion battery impedance for onboard battery management. *eTransportation* **2021**, *7*, 100093. [CrossRef]

7. Yang, X.; Doyle-Davis, K.; Gao, X.; Sun, X. Recent progress and perspectives on designing high-performance thick electrodes for all-solid-state lithium batteries. *eTransportation* **2022**, *11*, 100152. [CrossRef]
8. Liao, C. Electrolytes and additives for batteries Part I: Fundamentals and insights on cathode degradation mechanisms. *eTransportation* **2020**, *5*, 100068. [CrossRef]
9. Tong, S.; Klein, M.P.; Park, J.W. On-line optimization of battery open circuit voltage for improved state-of-charge and state-of-health estimation. *J. Power Sources* **2015**, *293*, 416–428. [CrossRef]
10. Ablay, G. Online Condition Monitoring of Battery Systems with a Nonlinear Estimator. *IEEE Trans. Energy Convers.* **2014**, *29*, 232–239. [CrossRef]
11. Mukherjee, N.; De, D. A New State-of-Charge Control Derivation Method for Hybrid Battery Type Integration. *IEEE Trans. Energy Convers.* **2017**, *32*, 866–875. [CrossRef]
12. Hossain, M.; Saha, S.; Haque, M.E.; Arif, M.T.; Oo, A.M.T. A Parameter Extraction Method for the Thevenin Equivalent Circuit Model of Li-ion Batteries. In Proceedings of the 2019 IEEE Industry Applications Society Annual Meeting, Baltimore, MD, USA, 29 September–3 October 2019.
13. Jaguemont, J.; Nikolian, A.; Omar, N.; Goutam, S.; Mierlo, J.V.; Bossche, P.V.d. Development of a Two-Dimensional-Thermal Model of Three Battery Chemistries. *IEEE Trans. Energy Convers.* **2017**, *32*, 1447–1455. [CrossRef]
14. Thirugnanam, K.; Joy T.P., E.R.; Singh, M.; Kumar, P. Mathematical Modeling of Li-Ion Battery Using Genetic Algorithm Approach for V2G Applications. *IEEE Trans. Energy Convers.* **2014**, *29*, 332–343. [CrossRef]
15. Zheng, Y.; Qin, C.; Lai, X.; Han, X.; Xie, Y. A novel capacity estimation method for lithium-ion batteries using fusion estimation of charging curve sections and discrete Arrhenius aging model. *Appl. Energy* **2019**, *251*, 113327. [CrossRef]
16. Sun, T.; Xu, B.; Cui, Y.; Feng, X.; Han, X.; Zheng, Y. A sequential capacity estimation for the lithium-ion batteries combining incremental capacity curve and discrete Arrhenius fading model. *J. Power Sources* **2021**, *484*, 229248. [CrossRef]
17. Yang, H.; Wang, P.; An, Y.; Shi, C.; Sun, X.; Wang, K.; Zhang, X.; Wei, T.; Ma, Y. Remaining useful life prediction based on denoising technique and deep neural network for lithium-ion capacitors. *eTransportation* **2020**, *5*, 100078. [CrossRef]
18. Goh, T.; Park, M.; Seo, M.; Kim, J.G.; Kim, S.W. Capacity estimation algorithm with a second-order differential voltage curve for Li-ion batteries with NMC cathodes. *Energy* **2017**, *135*, 257–268. [CrossRef]
19. Li, X.; Wang, Z.; Yan, J. Prognostic health conditio n for lithium battery using the partial incremental capacity and Gaussian process regression. *J. Power Sources* **2019**, *421*, 56–67. [CrossRef]
20. Li, X.; Wang, Z.; Zhang, L.; Zou, C.; Dorrell, D.D. State-of-health estimation for Li-ion batteries by combing the incremental capacity analysis method with grey relational analysis. *J. Power Sources* **2019**, *410–411*, 106–114. [CrossRef]
21. Tang, X.P.; Liu, K.L.; Lu, J.Y.; Liu, B.Y.; Wang, X.; Gao, F.R. Battery incremental capacity curve extraction by a two-dimensional Luenberger-Gaussian-moving-average filter. *Appl. Energy* **2020**, *280*, 115895. [CrossRef]
22. Berecibar, M.; Garmendia, M.; Gandiaga, I.; Crego, J.; Villarreal, I. State of health estimation algorithm of $LiFePO_4$ battery packs based on differential voltage curves for battery management system application. *Energy* **2016**, *103*, 784–796. [CrossRef]
23. Ni, Y.; Xu, J.; Zhu, C.; Pei, L. Accurate residual capacity estimation of retired $LiFePO_4$ batteries based on mechanism and data-driven model. *Appl. Energy* **2022**, *305*, 117922. [CrossRef]
24. Li, R.; Wang, H.; Dai, H.; Hong, J.; Tong, G.; Chen, X. Accurate state of charge prediction for real-world battery systems using a novel dual-dropout-based neural network. *Energy* **2022**, *250*, 123853. [CrossRef]
25. Xiong, R.; Yu, Q.; Wang, L.Y.; Lin, C. A novel method to obtain the open circuit voltage for the state of charge of lithium ion batteries in electric vehicles by using H infinity filter. *Appl. Energy* **2017**, *207*, 346–353. [CrossRef]
26. Wei, K.X.; Chen, Q.Y. Battery SOC Estimation based on Multi-model Adaptive Kalman Filter. In *Advanced Materials Research*; Trans Tech Publications Ltd.: Wollerau, Switzerland, 2012.
27. Ilies, A.I.; Chindris, G.; Pitica, D. A Comparison between State of Charge Estimation Methods: Extended Kalman Filter and Unscented Kalman Filter. In Proceedings of the 2020 IEEE 26th International Symposium for Design and Technology in Electronic Packaging (Siitme 2020), Pitesti, Romania, 21–24 October 2020; pp. 376–381.
28. Liu, X.; Chen, Z.; Zhang, C.; Wu, J. A novel temperature-compensated model for power Li-ion batteries with dual-particle-filter state of charge estimation. *Appl. Energy* **2014**, *123*, 263–272. [CrossRef]
29. He, Y.; Liu, X.; Zhang, C.; Chen, Z. A new model for State-of-Charge (SOC) estimation for high-power Li-ion batteries. *Appl. Energy* **2013**, *101*, 808–814. [CrossRef]
30. Zhou, Z.; Cui, Y.; Kong, X.; Li, J.; Zheng, Y. A fast capacity estimation method based on open circuit voltage estimation for $LiNi_xCo_yMn_{1-x-y}$ battery assessing in electric vehicles. *J. Energy Storage* **2020**, *32*, 101830. [CrossRef]
31. Yu, Q.Q.; Wan, C.J.; Li, J.F.; E, L.; Zhang, X.; Huang, Y.H.; Liu, T. An Open Circuit Voltage Model Fusion Method for State of Charge Estimation of Lithium-Ion Batteries. *Energies* **2021**, *14*, 1797. [CrossRef]
32. Yang, Y.P.; Liu, J.J.; Tsai, C.H. Improved estimation of residual capacity of batteries for electric vehicles. *J. Chin. Inst. Eng.* **2008**, *31*, 313–322. [CrossRef]
33. Dewangga, B.R.; Herdjunanto, S.; Cahyadi, A. Unknown Input Observer for Battery Open Circuit Voltage Estimation: An LMI Approach. In Proceedings of the 2018 the 10th International Conference on Information Technology and Electrical Engineering (icitee), Bali, Indonesia, 24–26 July 2018; pp. 471–475.

34. Zhu, J.G.; Wang, Y.X.; Huang, Y.; Gopaluni, R.B.; Cao, Y.K.; Heere, M.; Muhlbauer, M.J.; Mereacre, L.; Dai, H.F.; Liu, X.H.; et al. Data-driven capacity estimation of commercial lithium-ion batteries from voltage relaxation. *Nat. Commun.* **2022**, *13*, 1–10. [CrossRef]
35. Galushkin, N.E.; Yazvinskaya, N.N.; Galushkin, D.N. Model of Relaxation Processes in Batteries. *ECS Electrochem. Lett.* **2015**, 94–96. [CrossRef]
36. Kirk, T.L.; Please, C.P.; Chapman, S.J. Physical Modelling of the Slow Voltage Relaxation Phenomenon in Lithium-Ion Batteries. *J. Electrochem. Soc.* **2021**, *168*, 060554. [CrossRef]
37. Yang, J.; Du, C.Y.; Wang, T.; Gao, Y.Z.; Cheng, X.Q.; Zuo, P.J.; Ma, Y.L.; Wang, J.J.; Yin, G.P.; Xie, J.Y.; et al. Rapid Prediction of the Open-Circuit-Voltage of Lithium Ion Batteries Based on an Effective Voltage Relaxation Model. *Energies* **2018**, *11*, 3444. [CrossRef]
38. Huang, C.; Wang, L. Gaussian process regression-based modelling of lithium-ion battery temperature-dependent open-circuit-voltage. *Electron. Lett.* **2017**, *53*, 1214–1216. [CrossRef]